Surface-Tuned Electron Transfer and Electrocatalysis of Hexameric Tyrosine-Coordinated Heme Protein (HTHP)

ARTICLE *in* CHEMISTRY - A EUROPEAN JOURNAL · MARCH 2015

Impact Factor: 5.73 · DOI: 10.1002/chem.201405932

10 AUTHORS, INCLUDING:

Tillmann Utesch
Technische Universität Berlin
24 PUBLICATIONS **235** CITATIONS
SEE PROFILE

Aysu Yarman
Universität Potsdam
23 PUBLICATIONS **62** CITATIONS
SEE PROFILE

Andrea Mroginski
Technische Universität Berlin
72 PUBLICATIONS **1,084** CITATIONS
SEE PROFILE

Ulla Wollenberger
Universität Potsdam
173 PUBLICATIONS **3,491** CITATIONS
SEE PROFILE

ChemPubSoc Europe

DOI: 10.1002/chem.201405932

CHEMISTRY
A European Journal
Full Paper

Heme Proteins

Surface-Tuned Electron Transfer and Electrocatalysis of Hexameric Tyrosine-Coordinated Heme Protein (HTHP)

Lei Peng,[a] Tillmann Utesch,[b] Aysu Yarman,[a, d] Jae-Hun Jeoung,[c] Silke Steinborn,[c] Holger Dobbek,[c] Maria Andrea Mroginski,[b] Johannes Tanne,[d] Ulla Wollenberger,[a] and Frieder W. Scheller*[a, d]

Abstract: Molecular modeling, electrochemical methods, and quartz crystal microbalance were used to characterize immobilized hexameric tyrosine-coordinated heme protein (HTHP) on bare carbon or on gold electrodes modified with positively and negatively charged self-assembled monolayers (SAMs), respectively. HTHP binds to the positively charged surface but no direct electron transfer (DET) is found due to the long distance of the active sites from the electrode surfaces. At carboxyl-terminated surfaces, the neutrally charged bottom of HTHP can bind to the SAM. For this "disc" orientation all six hemes are close to the electrode and their direct electron transfer should be efficient. HTHP on all negatively charged SAMs showed a quasi-reversible redox behavior with rate constant k_s values between 0.93 and 2.86 s^{-1} and apparent formal potentials $E^{0'}_{app}$ between -131.1 and -249.1 mV. On the MUA/MU-modified electrode, the maximum surface concentration corresponds to a complete monolayer of the hexameric HTHP in the disc orientation. HTHP electrostatically immobilized on negatively charged SAMs shows electrocatalysis of peroxide reduction and enzymatic oxidation of NADH.

Introduction

The development of aerobic life on Earth required the evolution of enzymes able to degrade reactive oxygen species such as hydrogen peroxide and superoxide. The hexameric tyrosine-coordinated heme protein (HTHP) from the marine bacterium *Silicibacter pomeroyi* has a small hexameric, ringlike structure, in which each monomer consists of 76 amino acids and one heme group.[1] The molecular weight of the hexamer is 54 kDa. All six monomers are structurally equivalent and contain non-covalently bound heme groups. Each heme group is surrounded by three helices with heme-to-heme distances to its closest two neighbors of 18 Å. The iron is coordinated by a tyrosine residue in the proximal side, thus resembling the architecture of monofunctional heme-containing catalases. On the heme-distal side, HTHP is surrounded by arginine residues. The heme group is anchored in a hydrophobic patch, which stabilizes the vinyl and methyl groups of the heme, whereas the two propionate groups are accessible to the solvent. HTHP exhibits both peroxidatic and catalytic activities and thus has the potential to deactivate peroxide. In both pathways a sequence of redox reactions is involved. Interfacial electrochemistry of biological macromolecules can be utilized to elucidate the mechanism of the heterogeneous electron transfer (ET) and to analyze the enzymatic substrate conversion. According to the Marcus theory, the ET kinetics mainly depend on the distance between both redox sites.[2] That means an appropriate orientation of protein is essential to facilitate the ET. In this respect, alkyl thiol-contained self-assembled monolayers (SAMs) represent one of the most widely used approaches because this method can build up a highly ordered surface-bound molecular structure that makes the metal surfaces much more biocompatible.[3] Chemically tailored functionalities on SAMs have been used to achieve a "productive" orientation of the protein redox center towards the electrode surface, and the distance between the redox sites and the conducting surface can be varied by the length of carbon chain.[4]

In this paper, we describe the development of an electrode architecture for direct electrochemical communication with HTHP. The electrochemical behavior of the negatively charged HTHP was studied on positively charged and negatively charged alkyl thiol SAMs to elucidate the influence of the positively charged heme surroundings. Moreover, the effects of axial ligands and pH on the electrochemical response of HTHP

[a] Dr. L. Peng, Dr. A. Yarman, Prof. Dr. U. Wollenberger, Prof. Dr. F. W. Scheller
Institute of Biochemistry and Biology, Potsdam University
Karl-Liebknecht-Strasse 24–25, 14476 Potsdam (Germany)
Fax: (+49) 331 977-5050
E-mail: fschell@uni-potsdam.de

[b] Dr. T. Utesch, Dr. M. A. Mroginski
Institute of Chemistry, Technical University Berlin
Sekretariat PC 14, 10623 Berlin (Germany)

[c] Dr. J.-H. Jeoung, S. Steinborn, Prof. Dr. H. Dobbek
Institute of Biology, Structural Biology/Biochemistry
Humboldt Universität zu Berlin
Unter den Linden 6, 10099 Berlin (Germany)

[d] Dr. A. Yarman, J. Tanne, Prof. Dr. F. W. Scheller
Fraunhofer Institute
IZI-BB 14476 Potsdam (Germany)

Supporting information for this article is available on the WWW under http://dx.doi.org/10.1002/chem.201405932.

were examined. To characterize the enzymatic activity of the adsorbed HTHP, the bioelectrocatalysis in the presence of the co-substrate H_2O_2 and of the substrate nicotinamide adenine dinucleotide (NADH) was studied.

Results and Discussion

Modeling of HTHP binding on SAMs

The isoelectric point of HTHP was calculated to be 5.6, so the overall charge of HTHP at pH 8 should be negative. However, according to the surface electrostatic potential, the hexamer is positive in the middle around the active-site cavities owing to three conserved arginine residues in the direct vicinity, negative at the top and neutral at the bottom.

Since HTHP carries both positive and negative charges, negatively and positively charged SAMs should bind HTHP in different orientations. 11-Mercapto-1-undecanoic acid (MUA), 3-mercaptopropionic acid (MPA), α-lipoic acid, 11-mercapto-1-undecanol (MU), and 6-amino-1-hexanethiol hydrochloride (6-AHT) were chosen to yield negatively charged, neutral, or positively charged surfaces, respectively. On these SAM-coated surfaces, three possible orientations of HTHP are shown (Figure 1).

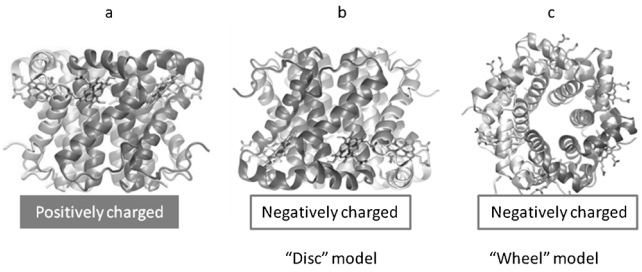

Figure 1. Postulated schematic representation of HTHP immobilized on a) positively charged SAM; b) "disc" model and c) "wheel" model on negatively charged SAMs.

To determine which parts of HTHP preferentially interact with differently charged SAMs, theoretical calculations were carried out. The plots were obtained by computing the interaction energy between the SAM surfaces and HTHP in different orientations by stepwise rotating the enzyme around the *x* axis (Φ angle) and the *y* axis (Ψ angle). On the positively charged surfaces, the most favorable geometry in interaction energy corresponds to the conformations of HTHP in which its dipole moment lies vertically relative to the surface. In this orientation, HTHP binds to the surface by means of a negatively charged patch. The six heme cofactors point away from the surface. Consequently, no or very slow electron transfer could be expected. Figure 2 shows the interaction energy landscapes of HTHP immobilized on carboxyl-terminated surfaces. On the negatively charged surfaces the energy landscape was relatively flat, which indicates that HTHP binds to the surface by means of neutrally charged sides, thus making the six heme groups point towards the surface. In this disc model (Figure 1b), the distance between the cofactors and the surfaces is shortest; hence, a fast electron transfer could be realized. Another orientation of binding, the "wheel" model (Figure 1c), could not be totally ruled out. In the "wheel" model, the binding happens through a positively charged patch on the side face of HTHP. The binding of HTHP in the wheel conformation is mediated by the interaction between the positively charged protein patch and the negatively charged SAM. The protein patch that surrounds the heme cofactor includes Lys20, Arg23, Lys27, Lys28, Arg36, and Arg40. The possibility of direct contact between the SAM and the heme is speculative and depends on the dynamics of the protein side chains.

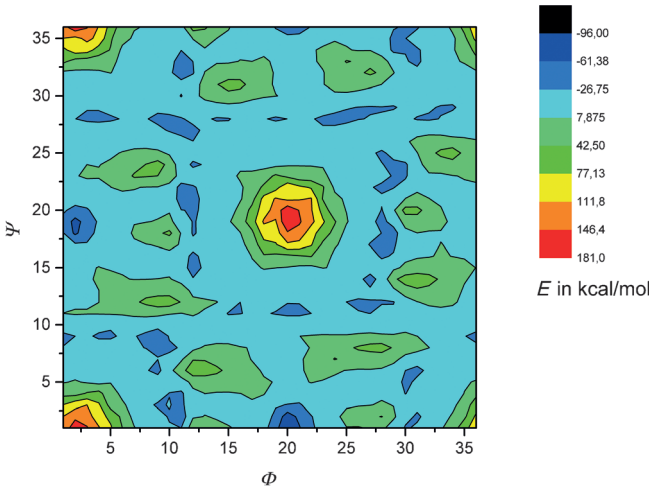

Figure 2. Interaction energy between HTHP and carboxyl-terminated SAMs obtained by rotating it stepwise around the *x* and *y* axes (Φ and Ψ angles).

HTHP immobilized on 6-amino-1-hexanethiol (6-AHT)-modified electrodes

The positively charged 6-AHT SAM was reported to facilitate the direct electron transfer (DET) of ferritin,[5] and, surprisingly, cytochrome c (cyt c) also.[6] Whereas free heme generated a couple of redox peaks, HTHP showed no redox signal between −0.5 and 0.2 V on the positively charged 6-AHT SAM. The addition of H_2O_2 (100 μM) led to no increase in the cathodic current. These results could be expected on the basis of the position of the active sites of HTHP. They are away from the negatively charged top, which interacted with 6-AHT SAM. Therefore, the long distance between the hemes and the electrode with this immobilization made electron transfer difficult and also prevented the electrocatalyis by HTHP.

Quartz crystal microbalance (QCM) experiments were carried out in parallel to determine whether HTHP could be adsorbed onto the 6-AHT-modified gold surface. Injection of an HTHP solution (5.2 μM in 1 mM tris(hydroxymethyl)aminomethane (Tris) buffer at pH 7) brought about an increase in the mass by the bound protein, which reached saturation after 3 h. The change in frequency of 20.02 Hz was used to calculate the loading of the protein to be 6.99 pmol cm^{-2} of hexameric protein according to the Sauerbrey equation.[7]

Direct electron transfer of HTHP on electrodes modified by negatively charged SAMs

In addition to bare glassy carbon and graphite, different SAMs were applied to modify gold electrodes: pure MUA, a mix of MUA/MU, MPA, and lipoic acid.

HTHP showed a well-pronounced pair of redox peaks on bare glassy carbon and graphite electrodes (see Figure S1 in the Supporting Information) and all gold electrodes covered with a negatively charged SAM (Figure 3a), whereas in the absence of HTHP, neither bare gold electrodes nor SAM-modified electrodes gave redox signals in the control experiments (Figure 3b). Since no HTHP electrochemistry was observed with the pure MU SAM (data not shown), the carboxylic groups of the SAMs are necessary for the productive orientation of HTHP. The appearance of a single peak pair in the cyclic voltammograms shows that the reduction of the six hemes cannot be measured individually. This finding is in accordance with the model of Molina et al.[8] for the electron transfer of a multi-redox-center species with noninteracting or positively interacting centers. Both mechanisms seem possible for the disc orientation of HTHP in which the six structurally identical heme groups have the same distance to the electrode. According to Molina's model, the sixth heme will have a potential that is 91 mV more negative than the first for noninteracting redox centers. In the case of positively interacting hemes, the potential span of the subsequent reduction steps can be narrower; however, the electron transfer of the first or subsequent centers has to induce conformational changes that facilitate the subsequent electron-transfer steps.

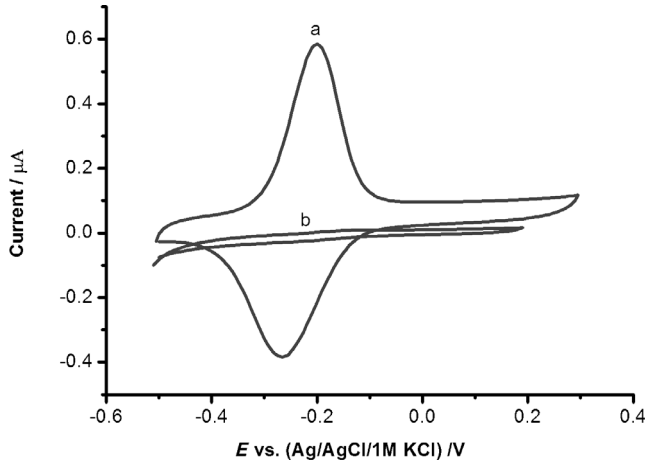

Figure 3. Cyclic voltammograms of HTHP immobilized on an MUA-modified gold electrode in 2.5 mM Tris buffer solution at pH 8 in the b) absence and a) presence of adsorbed HTHP at a scan rate of 100 mV s^{-1}.

Since the peaks in the cyclic voltammograms reflect a complex process, we call the means of the anodic and cathodic peak potentials the apparent formal potential $E^{0'}_{app}$ of HTHP. On electrodes modified with negatively charged SAMs, it was between −131 mV for the mixed SAM and −249 mV for lipoic acid versus Ag/AgCl 1 M KCl at pH 8.0 (Table 1). This pair of redox peaks is typical of the Fe^{2+}/Fe^{3+} redox couple of the heme group in proteins. To exclude the possibility of traces of free heme generating the peaks in the cyclic voltammograms, gold electrodes covered with either a SAM of MUA or a mixture of MUA and MU were incubated in heme-containing solutions. For both SAMs neither redox peaks in the potential region between −500 and +300 mV nor catalytic currents upon the addition of peroxide were observed. Therefore the peaks in the cyclic voltammograms represent the DET of the protein-bound heme and not that of free cofactor. The $E^{0'}_{app}$ of HTHP on negatively charged SAMs is considerably more negative than that for cytochrome c[9] on various SAMs. However, it is comparable to that of *b*-type heme proteins such as hemoglobin[10] and myoglobin[11] but more negative than for different cytochromes P450.[12]

The $E^{0'}_{app}$ of HTHP on pure MUA, MPA, and lipoic acid were comparable to each other, whereas the $E^{0'}_{app}$ for the MUA/MU SAM showed an anodic shift by approximately 110 mV. An explanation for the difference might be that the density of negative charges is much lower on the MUA/MU surface, which weakens the electrostatic interaction with the enzyme. This interpretation is in line with the finding that the apparent formal potential of HTHP is shifted in an anodic direction with increasing ionic strength (see Figure S3 in the Supporting Information). The negative shift upon HTHP binding to more anionic surfaces indicates that the ferric form binds more strongly than the ferrous form.

Table 1. Parameters of adsorption and DET of HTHP on different SAMs.

Electrode design	$E^{0'}_{app}$ [mV][a]	ΔE_p [mV][b]	Apparent k_s [s^{-1}][b]	Γ[c] [pmol cm^{-2}] CV[d]	QCM[e]
6-AHT	–	–	–	–	6.99
MUA/MU	−131.1 ± 5.7	85	0.93	1.13	1.30
MUA	−226 ± 1.3	85	2.86 ± 0.68	20.1	3.21
MPA	−203.4 ± 2.3	65	1.74 ± 0.3	15.7	
α-lipoic acid	−249.1 ± 6.7	75	1.21	12.1	

[a] $E^{0'}_{app}$ versus Ag/AgCl, 1 M, KCl. [b] ΔE_p and apparent k_s were determined at 100 mV s^{-1} in 2.5 mM Tris buffer at pH 8. [c] Amount (pmol) of hexameric HTHP in disc orientation ($n=6$) per cm^2 of geometric electrode area. [d] After adsorption from 1.3 mM HTHP in 50 mM Tris, pH 8, 150 mM NaCl. [e] During interaction with 5.2 μM HTHP.

Between pH 6 and 11, the reduction peaks of HTHP at MPA/Au are shifted in the cathodic direction by 53.3 mV per pH unit. This means that ionizable residues or ligands close to the redox center undergo changes in their protonation state.[13] The slope of the pH dependence is close to one-electron-/one-

proton-transfer process (see Figure S2 in the Supporting Information).

Small molecules like azides and cyanides have been reported to be typical inhibitors in heme-containing proteins by binding to the prosthetic group.[1,14] Sodium azide was chosen to study the binding to HTHP on MPA SAM. The addition of 0.22 mM sodium azide shifted the anodic and cathodic peaks by about 28 and 53 mV, respectively, in the anodic direction, which indicated that the azide bound more strongly to the ferrous form of the heme groups.

Surface concentration of electroactive HTHP

From the integration of the anodic peak, the surface coverage (Γ) of electrochemically active heme within the HTHP can be determined by using the equation $\Gamma = Q/nFA$, in which A is the area of the electrode (calculated to be 5.03 mm^2; see the Experimental Section), F is the Faraday constant, and n is the number of electrons for the redox process. Hexameric THP has a footprint for the flat adsorption of the disc of 17 nm × 17 nm ("disc" model; Figure 1b). Because all hemes have the same distance to the electrode surface, all six heme centers should contribute to the electron transfer. The surface concentration at saturation of a flat surface was estimated to be 0.56 pmol cm^{-2} for the hexameric protein, which is equivalent to 3.4 pmol cm^{-2} of heme. For the adsorption in the upright orientation of the HTHP, a surface concentration of 1.4 pmol cm^{-2} of the hexameric enzyme can be assumed at surface saturation ("wheel" model; Figure 1c). Because the distance between neighboring hemes is 1.8 nm, it is not certain that all six hemes will be "contacted" to the electrode. If all hemes were involved in the DET at surface saturation, 8.4 pmol cm^{-2} of heme would be expected.

For the MUA/MU SAM, the surface concentration of electroactive heme at saturation was determined to be 6.78 pmol cm^{-2}. This value is equivalent to either 1.13 pmol cm^{-2} of hexameric HTHP in "disc" orientation or 6.82 pmol cm^{-2} for the "wheel" model (with $n = 1$). Considering the surface roughness factor of two for the gold electrode,[15] the surface coverage obtained from cyclic voltammograms is comparable to the calculated value for a monolayer of HTHP in the "disc" orientation, which implies that all six hemes communicate with the electrode. For comparison, the surface concentration of a monolayer of cytochrome c (with a size of 10.2 nm^2), immobilized on the same MUA/MU SAM, was reported to be 9.2 pmol cm^{-2}.[4b]

When pure MUA was used to form a negatively charged SAM (HTHP-MUA-Au), the cyclic voltammograms displayed a pair of almost symmetric peaks with equal heights for the reduction and the oxidation, thus no HTHP was desorbed from the electrode during the oxidation/reduction cycle (Figure 3). The $E^{0'}_{app}$ of HTHP at MUA-modified electrodes was estimated to be (-226 ± 1.3) mV versus Ag/AgCl 1 M KCl at pH 8.0. On the basis of the anodic peak, the surface coverage (Γ) of electrochemically active heme was determined to be 121.2 pmol cm^{-2}, which is equivalent to 20.2 pmol cm^{-2} for the "disc" orientation of hexameric HTHP. These surface coverage values are much larger than those on MUA/MU SAM and also larger than that predicted from the calculated monolayer.

QCM experiments were carried out in parallel to compare the adsorption of HTHP on MUA/MU and pure MUA SAMs. On MUA-modified electrodes, the surface concentrations after interaction with 5.2 or 13 μM HTHP were comparable (see Figure S4 in the Supporting Information) and they exceeded the value for a complete monolayer. However, on MUA/MU-modified surfaces, the loading of hexameric HTHP reached 2 pmol cm^{-2}, a value that is close to the complete monolayer. These results confirm that HTHP adsorbed much more strongly on MUA SAM than on the mixed MUA/MU layer.

Kinetics of ET

Between 0.005 and 1.2 $V s^{-1}$ the cyclic voltammograms of HTHP-MUA-Au are almost symmetric with equal heights for the reduction and the oxidation peak with peak separations ΔE_p of 60 mV at scan rates of 100 mV s^{-1}, which is a characteristic of quasi-reversible systems. At low scan rates, from 0.005 to 0.05 V s^{-1}, both anodic and cathodic peak currents increase linearly with increasing scan rates, which indicates a surface-controlled electrode process (Figure 4, inset). The calculation of k_s for electron transfer between SAM-coated Au electrode and the attached HTHP (Table 1) was performed through the evaluation of the peak potential as function of the scan rate according to Laviron.[16]

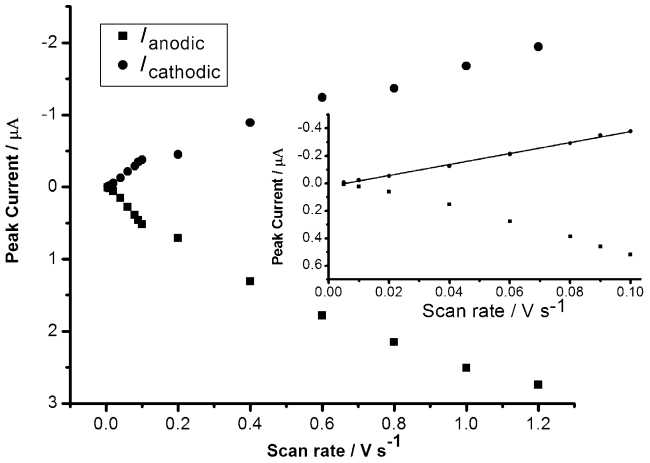

Figure 4. Scan rate dependency of the peak current for HTHP immobilized on an MUA-modified gold electrode in 2.5 mM Tris buffer solution at pH 8. Inset: from 5 to 100 mV s^{-1}.

However, at higher scan rates, neither anodic nor cathodic peak currents increased linearly with increasing scan rates or square roots of scan rates. A very similar behavior in terms of the frequency dependence was found for HTHP adsorbed onto the mixed SAM of MU/MUA in which a monolayer process is probable. Deviations from linear dependence of the peak current on the scan rate, possibly indicating a diffusion-controlled process, might not involve the protein directly; rather, this

might be due to diffusion-controlled efflux of ions necessary to maintain protein counter-ion charge balance.

Electrocatalysis of hydrogen peroxide reduction

HTHP is a bifunctional catalase–peroxidase enzyme. In the catalase mode, it degrades hydrogen peroxide into water and oxygen, and in the peroxidase mode, it follows the classic peroxidase reaction of oxidative dehydrogenation. For both reactions, the first phase of the catalytic cycle is the oxidation of HTHP by hydrogen peroxide to a compound I intermediate, which is a key oxidizing intermediate in the enzymatic reactions.[17]

There was no catalytic H_2O_2 reduction response for the control in the absence of HTHP (not shown). HTHP electrostatically immobilized on the negatively charged MUA SAM catalyzed the cathodic reduction of hydrogen peroxide. However, the bioelectrocatalytic reduction of H_2O_2 was not realized when HTHP was immobilized on MUA/MU SAM. This finding is in line with a low surface concentration of HTHP.

The catalytic current of HTHP at the MUA-modified electrode increased linearly in the range from 1 to 32 μM with increasing concentrations of H_2O_2 (Figure 5). It started from around

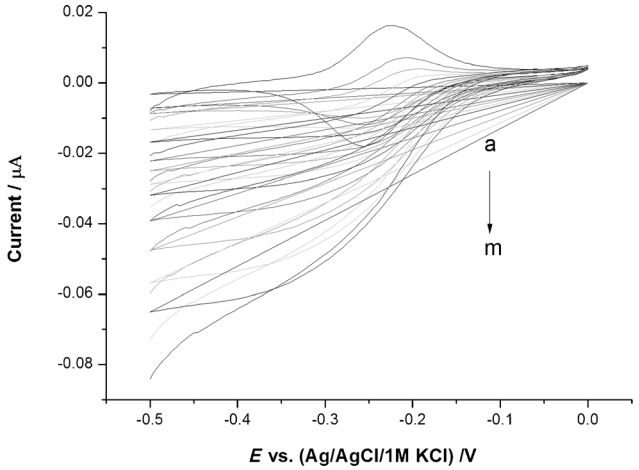

Figure 5. Cyclic voltammograms of HTHP on MUA SAM in 2.5 mM Tris pH 8 for different H_2O_2 concentrations: a–m) 0, 1, 2, 4, 6, 8, 10, 12, 14, 17, 20, 23, 27, and 32 μM. The scan rate was 5 mV s^{-1}.

−0.1 V upon addition of hydrogen peroxide (Figure 5), which is 650 mV more negative than that determined for the reaction compound I/compound II of horseradish peroxidase (HRP).[17a] Since no mediator took part, the reduction current arose from DET between the electrode and the hemes of HTHP.[18] The formation of a compound I analogue in the HTHP cycle should lead to the formation of catalytic currents starting around 600 mV versus SCE. In several papers for HRP-modified carbon, gold, tin oxide, platinum, and indium tin oxide (ITO) electrodes the cathodic reduction starts between 200 and 400 mV versus SCE. This behavior has been ascribed to a combination of direct electron transfer from compound I and the action of redox-active groups at the electrode surface as mediators. In fact, the pretreatment of the electrode surface has a significant effect on the catalytic peroxide reduction. However, there are several reports on different heme-protein-modified electrodes that describe the peroxide reduction at the potential in which the heme is in the reduced state. In analogy to unfolded cytochrome c,[19] the reaction with peroxide could lead through Fe^{II} to Fe^{IV}=O for HTHP as well.[20] This species has a remarkably more positive formal potential than the ferric heme and it is immediately reduced at this potential along with the reduction of ferric HTHP.

Peroxide-dependent oxidation of NADH

Although the physiological substrates are still unknown, several organic electron donors were found to be substrates for HTHP such as NAD(P)H, pyrogallol, and *o*-dianisidine. HTHP displays different degrees of peroxidase activities towards these substrates depending on pH values: NAD(P)H at physiological pH values, pyrogallol at pH 11.7, and *o*-dianisidine at 7.5. Among them, NADH is the best substrate under physiological conditions[1] and could be oxidized by HTHP.

The HTHP-catalyzed oxidation of NADH in the presence of H_2O_2 under basic conditions (pH 8) was selected to demonstrate the enzymatic activity of HTHP immobilized on negatively charged SAMs. To prevent the destruction of heme by peroxide, we applied a low concentration. Since 10 μM peroxide was effective for the electrocatalysis of hydrogen peroxide reduction, this concentration was used in the following experiments. The currents for the cathodic reduction of peroxide gradually decrease with the increase in NADH concentration (Figure 6b–k), which reflects the consumption of H_2O_2. The height of the peaks are linearly dependent on the NADH concentration in the range from 0 to 4 μM and reaches the saturation state at around 12 μM of NADH, which agrees with the theoretical stoichiometry of 1:1 between H_2O_2 and NADH.

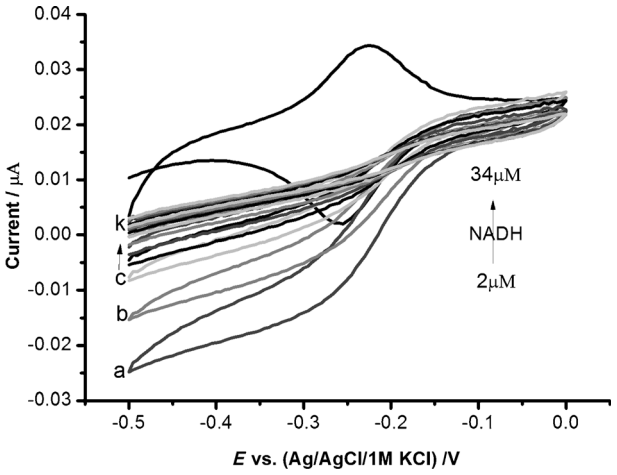

Figure 6. Cyclic voltammograms of HTHP on MUA SAM in 2.5 mM Tris pH 8 for different NADH concentrations in the presence of a) 10 μM H_2O_2 and b–k) 2, 4, 6, 8, 10, 12, 14, 18, 22, 28, and 34 μM. The scan rate was 5 mV s^{-1}.

Conclusion

For multi-center redox enzymes, the orientation of the molecule is crucial for effective reactions at interfaces such as membranes but also at electrodes. This fact is well understood for proteins that possess different redox centers, for example, cellobiose dehydrogenase, sulfite oxidase, and FeS-contaning hydogenases, because in most cases only heme groups or FeS clusters can directly communicate with the electrode.

For the homo-hexamer HTHP all six redox centers are uniformly distributed on the cover of the wheel-shaped molecule. The combination of electrochemical and QCM investigations with theoretical modeling of possible orientations of the hexamer on the electrode surface revealed that the charge of the surface is crucial. On electrodes modified with positively charged SAMs, the protein is adsorbed in a non-productive orientation for direct heterogeneous electron transfer and bioelectrocatalysis. The appearance of a single peak pair in the cyclic voltammograms on negatively charged SAMs with a surface concentration of electroactive HTHP that represents all hemes is in accordance with the model for the electron transfer of a multi-redox center species with noninteracting or positively interacting centers. Both mechanisms seem possible for the disc orientation of HTHP whereby the six structurally identical heme groups have the same distance to the electrode. For positively interacting heme the electron transfer of the first or subsequent centers has to induce conformational changes that facilitate the subsequent electron-transfer steps.

Experimental Section

Chemicals

Hydrogen peroxide (H_2O_2 30%), sodium azide, 11-mercapto-1-undecanoic acid (MUA), 11-mercapto-1-undecanol (MU), 3-mercaptopropionic acid (MPA), and 6-amino-1-hexanethiol hydrochloride (6-AHT) were purchased from Aldrich (Steinheim, Germany); α-lipoic acid, aniline, and hemin were from Sigma (Steinheim, Germany); NADH was from Gerbu (Gerbu Biotechnic GmbH), and Tris was from Serva (Germany). MUA, MU, MPA, and 6-AHT (5 mM) were all dissolved in 96% ethanol of analytical grade. α-Lipoic acid was prepared as a 5 mM stock solution in ethanol and freshly diluted with Millipore water to 1 mM. Tris buffers (2.5 mM, pH 5.5–11) with pH adjustment using acetic acid or NaOH were employed for the electrochemical studies. A gold wire with a diameter of 0.5 mm was purchased from Goodfellow (Bad Nauheim, Germany). AT-cut gold-coated QCM sensor chips (5 MHz) were purchased from Q-sense (Q-Sense AB, Sweden). All reagents were of analytical grade and used without further purification.

Enzyme preparation

Hexameric tyrosine-coordinated heme protein was prepared as described by Jeoung et al.[1] It was expressed in *Escherichia coli* Rosetta (DE3) by induction with 1 μM isopropyl β-D-1-thiogalactopyranoside (IPTG). HTHP (approximately 80 mg per liter of culture) was purified to homogeneity as determined by SDS-PAGE and native PAGE by using standard protein purification protocols. Purified HTHP showed a low rz value of 0.26 (ratio of absorbance at Soret peak and 280 nm), which was greatly improved by reconstitution of this preparation with equal molar ratios of hemin chloride, which finally gave an rz value 2.8. All further experiments were carried out with the reconstituted enzyme. The purified protein gave a single band of approximately 7.9 kDa on SDS-PAGE, whereas an apparent molecular mass of 54 kDa was determined by means of gel filtration chromatography on Superdex S-200 prep grade, which indicated that HTHP forms a hexamer in solution. The final concentration of the purified enzyme was 1.3 mmol L^{-1} in 50 mM Tris-HCl at pH 8 with 150 mM NaCl, and it was used for the electrochemical and physical characterization.

Modification of electrode

Gold wires with a diameter of 0.5 mm were boiled in 2 M KOH solution for 4 h and kept in concentrated HNO_3 for 10 min. After carefully rinsing with Millipore water, they were stored in concentrated H_2SO_4 when not in use. Before every usage, the electrodes were washed by Millipore water and kept in concentrated HNO_3 for 10 min, then rinsed by Millipore water again in each successive step.[21]

Cleaned electrodes were incubated in a mixture of 5 mM MUA and 5 mM MU with a volume ratio 1:3 at least overnight at 4 °C. MUA and MU were dissolved in 96% ethanol and freshly prepared each time before modification. After being washed by Millipore water, an MUA/MU-modified gold wire electrode was immersed directly in HTHP solution (1.3 mM) for 3 h at 4 °C. Pure MUA-, MPA-, 6-AHT-, and lipoic acid-modified HTHP electrodes were prepared in the same way as described above for MUA/MU modification. All regents were dissolved in ethanol and freshly prepared each time before modification.

AT-cut gold-coated QCM sensor crystals were cleaned in a mixture of 5:1:1 of water, ammonia (25%), and hydrogen peroxide, heated to 75–80 °C for 5–10 min, rinsed with ultrapure water, and then dried with nitrogen gas. The cleaned crystals were incubated in a mixture of 5 mM MUA and 5 mM MU with a volume ratio 1:3 or 5 mM pure MUA at least overnight at 4 °C. MUA and MU were dissolved in ethanol and freshly prepared each time before modification. After washing with Millipore water, an MUA/MU- or MUA-modified sensor crystal was dried with nitrogen gas and gently placed onto the flow modules, which were ready for running the experiments.

Apparatus and measurements

Electrochemical measurements were carried out using a PalmSens electrochemical station. A three-electrode system with a working electrode, a Pt wire as the counter electrode, and Ag/AgCl (KCl, 1 M) as the reference electrode, unless otherwise noted, was used in all electrochemical experiments. Both cyclic voltammetry (CV) and SWV were conducted in a 2 mL compartment of a custom-built reaction chamber with an adjustable magnetic stirring system. All experiments were performed at room temperature (25 °C) with exclusion of oxygen. Cyclic voltammograms were recorded in 2.5 mM Tris (2 mL, pH 8). All electrodes were scanned in the range from −0.5 to +0.2 V with different scan rates.

The surface areas of gold wire electrodes were determined by CV in $K_3Fe(CN)_6$ solution (0.75 M) with KCl (1 M).

QCM was conducted to study the real-time binding of HTHP on pure MUA-, MUA/MU-, and 6-AHT-modified gold-coated QCM sensor chips by using a Q-Sense E4 instrument (Q-Sense AB, Sweden). All binding measurements were performed in either 1 mM Tris buffer at pH 7 or 50 mM Tris-HCl with 150 mM NaCl at

pH 8 with a flow rate of 10 μL min^{-1} at 25 °C. The buffer solution was first injected by an automatic pump until a steady baseline was obtained and reached equilibrium. Stock HTHP solution (1.3 mM) was diluted to 5.2 or 13 μM by 1 mM Tris buffer at pH 7 or 50 mM Tris-HCl with 150 mM NaCl at pH 8. Then the protein solutions were injected until they reached a saturation state. The protein-free buffer was subsequently injected to remove the unbound proteins. All QCM data were processed in Q-Tools software which is included in the E4 system.

System setup for theoretical calculation

Coordinates for HTHP were extracted from the crystallographic structure (pdb entry: 2oyy),[1] and the structure was protonated according to pH 7.0. For the following calculations (dipole moment, potential-energy surface, and interaction energy) the CHARMM27 force field[22] was used. The amino-terminated SAM was constructed and protonated (pH 7.0) as described in the literature,[23] and the HEME cofactors were treated with the CHARMM parameter set.[22]

Dipole moment

The dipole moment was calculated with VMD1.9.1[24] using the charge distribution described by the partial charges of the CHARMM27 force field.

Potential-energy surface

The potential-energy surface was calculated with the APBS tool.[25]

Interaction energy landscape

To identify interaction hotspots of HTHP with amino- and carboxyl-terminated SAMs an interaction energy sampling was carried out. Protonated HTHP was placed on the corresponding surface in a certain orientation, and the interaction energy was calculated as described in the following manner. The orientation of HTHP was described by two angles, θ and Ψ, which describe the surface plane. During the sampling, θ and Ψ were systematically varied in 10° steps from 0 to 350° to obtain all possible combinations. For each angle pair, HTHP was rotated according to the two angles and placed in a 5 Å separation distance to the SAM. In these conformations the interaction energy was calculated with the NAMD Energy Tool available in VMD1.9.1.[24]

Acknowledgements

The work is a part of UniCat, the Cluster of Excellence in the field of catalysis coordinated by the Technical University of Berlin and financially supported by Deutsche Forschungsgemeinschaft (DFG) within the framework of the German Excellence Initiative (EXC 314).

Keywords: electrochemistry · electron transfer · heme proteins · molecular modeling · monolayers

[1] J.-H. Jeoung, D. A. Pippig, B. M. Martins, N. Wagener, H. Dobbek, *J. Mol. Biol.* **2007**, *368*, 1122 – 1131.

[2] a) R. A. Marcus, *Angew. Chem. Int. Ed. Engl.* **1993**, *32*, 1111 – 1121; *Angew. Chem.* **1993**, *105*, 1161 – 1172; b) R. A. Marcus, N. Sutin, *Biochim. Biophys. Acta Rev. Bioenerg.* **1985**, *811*, 265 – 322.

[3] a) G. M. Whitesides, A. Kumar, H. A. Biebuyck, N. L. Abbott, P. A. Dimilla, *Abstr. Pap. Am. Chem. Soc.* **1994**, *207*, 373-PHYS; b) J. Rickert, T. Weiss, W. Kraas, G. Jung, W. Gopel, *Biosens. Bioelectron.* **1996**, *11*, 591 – 598; c) L. X. Tiefenauer, S. Kossek, C. Padeste, P. Thiebaud, *Biosens. Bioelectron.* **1997**, *12*, 213 – 223.

[4] a) L. Jiang, A. Glidle, C. J. McNeil, J. M. Cooper, *Biosens. Bioelectron.* **1997**, *12*, 1143 – 1155; b) B. Ge, F. Lisdat, *Anal. Chim. Acta* **2002**, *454*, 53 – 64.

[5] M. Tominaga, K. Miyahara, K. Soejima, S. Nomura, M. Matsumoto, I. Taniguchi, *J. Colloid Interface Sci.* **2007**, *313*, 135 – 140.

[6] G. X. Wang, M. Wang, Z. Q. Wu, W. J. Bao, Y. Zhou, X. H. Xia, *Analyst* **2013**, *138*, 5777 – 5782.

[7] K. A. Marx, *Biomacromolecules* **2003**, *4*, 1099 – 1120.

[8] A. Molina, C. Serna, M. López-Tenés, M. M. Moreno, *J. Electroanal. Chem.* **2005**, *576*, 9 – 19.

[9] a) S. Song, R. A. Clark, E. F. Bowden, M. J. Tarlov, *J. Phys. Chem.* **1993**, *97*, 6564 – 6572; b) A. Avila, B. W. Gregory, K. Niki, T. M. Cotton, *J. Phys. Chem. B* **2000**, *104*, 2759 – 2766; c) D. H. Waldeck, D. E. Khoshtariya, in *Modern Aspects of Electrochemistry: Applications of Electrochemistry and Nanotechnology in Biology and Medicine, Vol. 1* (Ed.: N. Eliaz), , Springer, New York, **2011**, 52.

[10] a) Z. Mai, X. Zhao, Z. Dai, X. Zou, *Talanta* **2010**, *81*, 167 – 175; b) H. Sun, H. Y. Ma, N. F. Hu, *Bioelectrochem. Bioenerg.* **1999**, *49*, 1 – 10.

[11] S. Ray, S. Chand, Y. Zhang, S. Nussbaum, K. Rajeshwar, R. Perera, *Electrochim. Acta* **2013**, *99*, 85 – 93.

[12] a) M. L. Yang, J. L. Kabulski, L. Wollenberg, X. Q. Chen, M. Subramanian, T. S. Tracy, D. Lederman, P. M. Gannett, N. Q. Wu, *Drug Metab. Dispos.* **2009**, *37*, 892 – 899; b) A. Fantuzzi, E. Capria, L. H. Mak, V. R. Dodhia, S. J. Sadeghi, S. Collins, G. Somers, E. Hug, G. Gilardi, *Anal. Chem.* **2010**, *82*, 10222 – 10227.

[13] A. Lindgren, T. Larsson, T. Ruzgas, L. Gorton, *J. Electroanal. Chem.* **2000**, *494*, 105 – 113.

[14] a) M. Tatarko, J. A. Bumpus, *Arch. Biochem. Biophys.* **1997**, *339*, 200 – 209; b) O. M. Lardinois, P. G. Rouxhet, *Biochim. Biophys. Acta-Protein Struct. Mol. Enzymol.* **1996**, *1298*, 180 – 190.

[15] D. D. Schlereth, E. Katz, H. L. Schmidt, *Electroanalysis* **1995**, *7*, 46 – 54.

[16] E. Laviron, *J. Electroanal. Chem.* **1979**, *101*, 19 – 28.

[17] a) E. Csöregi, G. Jonssonpettersson, L. Gorton, *J. Biotechnol.* **1993**, *30*, 315 – 337; b) L. Gorton, G. Jonssonpettersson, E. Csoregi, K. Johansson, E. Dominguez, G. Markovarga, *Analyst* **1992**, *117*, 1235 – 1241.

[18] a) G. Jönsson, L. Gorton, *Electroanalysis* **1989**, *1*, 465 – 468; b) G. Presnova, V. Grigorenko, A. Egorov, T. Ruzgas, A. Lindgren, L. Gorton, T. Borchers, *Faraday Discuss.* **2000**, *116*, 281 – 289.

[19] A. Ranieri, G. Battistuzzi, M. Borsari, C. A. Bortolotti, G. Di Rocco, S. Monari, M. Sola, *Electrochem. Commun.* **2012**, *14*, 29 – 31.

[20] H. B. Dunford, *Coord. Chem. Rev.* **2002**, *233*, 311 – 318.

[21] S. Frasca, O. Rojas, J. Salewski, B. Neumann, K. Stiba, I. M. Weidinger, B. Tiersch, S. Leimkuehler, J. Koetz, U. Wollenberger, *Bioelectrochem.* **2012**, *87*, 33 – 41.

[22] A. D. MacKerell, D. Bashford, M. Bellott, R. L. Dunbrack, J. D. Evanseck, M. J. Field, S. Fischer, J. Gao, H. Guo, S. Ha, D. Joseph-McCarthy, L. Kuchnir, K. Kuczera, F. T. K. Lau, C. Mattos, S. Michnick, T. Ngo, D. T. Nguyen, B. Prodhom, W. E. Reiher III, B. Roux, M. Schlenkrich, J. C. Smith, R. Stote, J. Straub, M. Watanabe, J. Wiorkiewicz-Kuczera, D. Yin, M. Karplus, *J. Phys. Chem. B* **1998**, *102*, 3586 – 3616.

[23] T. Utesch, D. Millo, M. A. Castro, P. Hildebrandt, I. Zebger, M. A. Mroginski, *Langmuir* **2013**, *29*, 673 – 682.

[24] W. Humphrey, A. Dalke, K. Schulten, *J. Mol. Graphics* **1996**, *14*, 33 – 38.

[25] N. A. Baker, D. Sept, S. Joseph, M. J. Holst, J. A. McCammon, *Proc. Natl. Acad. Sci. USA* **2001**, *98*, 10037 – 10041.

Received: November 3, 2014
Published online on ■■ ■■, 0000

FULL PAPER

Heme Proteins

*L. Peng, T. Utesch, A. Yarman, J.-H. Jeoung, S. Steinborn, H. Dobbek, M. A. Mroginski, J. Tanne, U. Wollenberger, F. W. Scheller**

■■ – ■■

Surface-Tuned Electron Transfer and Electrocatalysis of Hexameric Tyrosine-Coordinated Heme Protein (HTHP)

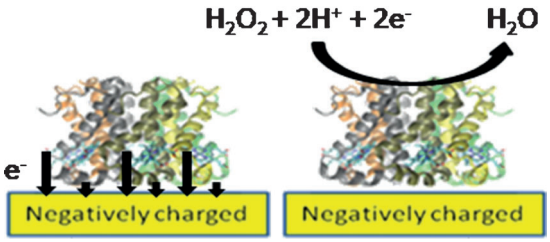

Heme theme: Electrochemistry and QCM were used to characterize hexameric tyrosine-coordinated heme protein (HTHP) immobilized on bare carbon or on Au electrodes modified by differently charged self-assembled monolayers. Experimental results are in line with theoretical calculations; HTHP at negatively charged surfaces shows both direct electron transfer of the heme centers and bioelectrocatalysis.